Soft Matter

PAPER

View Article Online
View Journal | View Issue

Cite this: *Soft Matter*, 2014, **10**, 8615

Are block copolymer worms more effective Pickering emulsifiers than block copolymer spheres?†

K. L. Thompson,* C. J. Mable, A. Cockram, N. J. Warren, V. J. Cunningham, E. R. Jones, R. Verber and S. P. Armes*

RAFT-mediated polymerisation-induced self-assembly (PISA) is used to prepare six types of amphiphilic block copolymer nanoparticles which were subsequently evaluated as putative Pickering emulsifiers for the stabilisation of *n*-dodecane-in-water emulsions. It was found that *linear* poly(glycerol monomethacrylate)–poly(2-hydroxypropyl methacrylate) (PGMA–PHPMA) diblock copolymer spheres and worms do not survive the high shear homogenisation conditions used for emulsification. Stable emulsions are obtained, but the copolymer acts as a polymeric surfactant; individual chains rather than particles are adsorbed at the oil–water interface. Particle dissociation during emulsification is attributed to the weakly hydrophobic character of the PHPMA block. Covalent stabilisation of these copolymer spheres or worms can be readily achieved by addition of ethylene glycol dimethacrylate (EGDMA) during the PISA synthesis. TEM studies confirm that the resulting *cross-linked* spherical or worm-like nanoparticles survive emulsification and produce genuine Pickering emulsions. Alternatively, stabilisation can be achieved by either replacing or supplementing the PHPMA block with the more hydrophobic poly(benzyl methacrylate) (PBzMA). The resulting *linear* spheres or worms also survive emulsification and produce stable *n*-dodecane-in-water Pickering emulsions. The intrinsic advantages of anisotropic worms over isotropic spheres for the preparation of Pickering emulsions are highlighted. The former particles are more strongly adsorbed at similar efficiencies compared to spheres and also enable smaller oil droplets to be produced for a given copolymer concentration. The scalable nature of PISA formulations augurs well for potential applications of anisotropic block copolymer nanoparticles as Pickering emulsifiers.

Received 4th August 2014
Accepted 12th September 2014

DOI: 10.1039/c4sm01724b

www.rsc.org/softmatter

Introduction

Pickering emulsions comprise oil or water droplets stabilised by solid particles and have been recognised for over a century.[1,2] Many different types of solid particles have been utilised as Pickering emulsifiers, such as inorganic clays,[3–6] silica[7–11] and polymer latex particles.[12] A layer of adsorbed particles surrounds each droplet to provide a strong steric barrier towards droplet coalescence, making Pickering emulsions far more stable than surfactant-stabilised emulsions. The energy of detachment for an individual particle adsorbed at the oil–water interface depends on both its three-phase contact angle and the particle radius, with significantly more energy being required to remove larger particles from the oil–water interface.[13] In practice, this detachment energy is often so large (> 1000 kT) that in some cases certain types of nanoparticles can be considered to be irreversibly adsorbed.[13,14]

Much of the growing literature on Pickering emulsions has focused on spherical particles. There are far fewer reports of the use of non-spherical Pickering emulsifiers based on rigid rods or flexible worms. Noble *et al.*[15] prepared so-called 'hairy' colloidosomes using relatively large (10–70 μm) 'microrods' prepared from a photocurable epoxy resin as the droplet stabiliser. In this case the hot aqueous phase contained 1.5 wt% agarose that gelled upon cooling, trapping the 'microrods' at the interface. Vermant and co-workers[16] used a multiple back-scattering technique to demonstrate that more stable Pickering emulsions are obtained when employing elongated polystyrene latexes with relatively high aspect ratios (with the original isotropic latex particles being used as a control). Similar results were also obtained with ellipsoidal hematite particles.[16] Guevara *et al.*[17] reported that 2D nanosheets can produce highly stable foams. Cellulose fibres have also been used to stabilise both water-in-oil and oil-in-water emulsions.[18–20] In this case the fibre aspect ratio strongly influenced the droplet surface coverage: short fibres led to densely-coated oil droplets (>80% coverage), whereas using longer fibres produced significantly lower surface coverages (~40%).[20]

Department of Chemistry, The University of Sheffield, Dainton Building, Brook Hill, Sheffield, South Yorkshire, S3 7HF, UK. E-mail: s.p.armes@sheffield.ac.uk

† Electronic supplementary information (ESI) available. See DOI: 10.1039/c4sm01724b

Recently, our group has reported the facile preparation of a range of diblock copolymer nanoparticles *via* polymerisation-induced self-assembly (PISA) using reversible addition–fragmentation chain transfer (RAFT) polymerisation in concentrated aqueous solution.[21,22] In the prototypical formulation, a water-soluble poly(glycerol monomethacrylate) (PGMA) chain transfer agent is used to grow a water-insoluble poly(2-hydroxypropyl methacrylate) (PHPMA) block, leading to the *in situ* formation of PGMA–PHPMA diblock copolymer nanoparticles *via* RAFT aqueous dispersion polymerisation.[23–25] In principle, the final particle morphology is simply dictated by the relative volume fractions of each block, although in practice the copolymer concentration can also play an important role.[26] This versatile route to block copolymer nanoparticles enables the efficient synthesis of spheres, worms or vesicles *directly in water at up to 25% solids*. Moreover, the surface properties of these nanoparticles can be tuned by judicious selection of the stabiliser for a given core-forming block,[27–31] which is likely to be of considerable interest when designing new bespoke Pickering emulsifiers.

Recently, we compared the Pickering emulsifier performance of linear and crosslinked PGMA–PHPMA block copolymer vesicles (also known as 'polymersomes') prepared using a PISA formulation.[32] One important finding was that use of an ethylene glycol dimethacrylate (EGDMA) cross-linker was essential to preserve the relatively delicate vesicular morphology during the high-shear homogenisation required to generate the oil droplets. In the absence of any EGDMA, the *linear* vesicles simply dissociated during homogenisation and the resulting emulsion droplets became stabilised by individual copolymer chains, rather than vesicles. In contrast, EGDMA-crosslinked vesicles survived the emulsification conditions and were able to function as the desired 'Pickering' emulsifier. In the present work, we explore whether covalent cross-linking is also essential to prevent dissociation of PGMA-based block copolymer spheres and worms when employed as putative Pickering emulsifiers. In particular, we emphasise that the block copolymer worms described herein are much more readily accessible on a multigram scale than the various anisotropic nanoparticles that have been explored to date.[15,16,18–20] Provided that conformal contact with the interface can be achieved, such worms are expected to be much more strongly adsorbed at the oil–water interface than the equivalent spherical nanoparticles. For example, if worm-like nanoparticles are sufficiently anisotropic (*i.e.* if their mean contour length L is much greater than the mean worm radius R), then their specific surface area, A_s, can be approximated by the equation: $A_s \sim 2/\rho R$, where ρ is the particle density and R is the mean worm radius (see ESI† for further details). In contrast, the spherical nanoparticles that undergo 1D fusion to form such worms during the PISA synthesis[24,27] have a specific surface area given by $A_s = 3/\rho r$, where r is the mean sphere radius and $r \sim R$. Thus the reduction in specific surface area that occurs on fusing multiple spheres to form each individual worm is only around 33%. To a good first approximation, the energy of attachment of a worm of radius R comprising x fused spheres at the oil–water interface is expected to be x times higher than the energy of attachment of an individual spherical nanoparticle of radius r. Thus the worm morphology affords a specific surface area comparable to that of the original spheres, but the former particles are much more strongly adsorbed at the oil–water interface. Hence the present study is focused on addressing the following fundamental question: do worm-like nanoparticles offer significant advantages as Pickering emulsifiers over their spherical nanoparticle precursors?

For the sake of brevity, we introduce a shorthand notation to describe the various diblock and triblock copolymers synthesised in this study such that G, H, B and E stand for glycerol monomethacrylate, 2-hydroxypropyl methacrylate, benzyl methacrylate and ethylene glycol dimethacrylate, respectively. For example, G_x–H_y–E_z indicates a poly(glycerol monomethacrylate-*block*-2-hydroxypropyl methacrylate-*block*-ethylene glycol dimethacrylate) triblock copolymer, where x, y and z indicate the mean degrees of polymerisation (DP) of each block.

Experimental

Materials

Glycerol monomethacrylate was obtained from GEO Specialty Chemicals (Hythe, UK) and was used as received. 2-Hydroxypropyl methacrylate, ethylene glycol dimethacrylate, 4,4′-azobis(4-cyanopentanoic acid) (ACVA), *n*-dodecane, and tolylene 2,4-diisocyanate-terminated poly(propylene glycol) (PPG-TDI) were purchased from Aldrich (UK) and were used as received, unless otherwise stated. 4-Cyano-4-(2-phenyl-ethanesulfanylthiocarbonyl)sulfanylpentanoic acid (PETTC) was prepared in-house as reported previously and *n*-hexane was purchased from Fisher.[31]

Synthesis of poly(glycerol monomethacrylate) macromolecular chain transfer agent (macro-CTA)

PGMA macro-CTAs with mean degrees of polymerisation of 37, 45, 51 and 100 (denoted G_{37}, G_{45}, G_{51} and G_{100}, respectively) were synthesised *via* RAFT polymerisation of glycerol monomethacrylate in ethanol at 70 °C, as described previously.[26]

Synthesis of linear G_{100}–H_{200} nanoparticles *via* RAFT aqueous dispersion polymerisation

G_{100} macro-CTA (0.5 g, 0.031 mmol), HPMA monomer (0.89 g, 6.16 mmol) ACVA (2.9 mg, 0.010 mmol, CTA/ACVA molar ratio = 3.0) and previously degassed deionised water (13.59 g, 10% w/w), were weighed into a 50 mL round-bottomed flask. The reaction solution was purged with N_2 for 30 min prior to immersion in an oil bath set at 70 °C. The reaction was stirred for 3 h at this temperature under a N_2 atmosphere prior to being quenched by exposure to air. Linear G_{45}–H_{100} diblock copolymer worms were prepared using the same protocol.

Synthesis of crosslinked G_{100}–H_{200}–E_{20} nanoparticles *via* RAFT aqueous dispersion polymerisation

G_{100} macro-CTA (0.5 g, 0.031 mmol), HPMA monomer (0.89 g, 6.16 mmol) ACVA (2.9 mg, 0.010 mmol, CTA/ACVA molar

ratio = 3.0) and previously degassed deionised water (13.59 g, 10% w/w), were weighed into a 50 mL round-bottomed flask. The reaction solution was purged with N_2 for 30 min prior to immersion in an oil bath set at 70 °C. The reaction mixture was stirred for 3 h at this temperature under a N_2 atmosphere prior to the addition of EGDMA cross-linker (0.122 g, 0.616 mmol). The colloidal dispersion was stirred overnight (16 h) to ensure complete EGDMA monomer conversion and the polymerisation was quenched by exposure to air. Crosslinked G_{45}–H_{100}–E_{10} worms were also prepared using the above protocol.

Synthesis of linear G_{51}–B_{250} nanoparticles *via* RAFT aqueous emulsion polymerisation

A typical protocol for the synthesis of $PGMA_{51}$–$PBzMA_{250}$ diblock copolymer was as follows: $PGMA_{51}$ macro-CTA (0.1702 g), BzMA (0.8904 g, 5.05 mmol), ACVA (1.40 mg, 4.99 μmol; CTA/ACVA molar ratio = 4.0) and water (7.97 g, 10% w/w) were weighed into a 25 mL round-bottom flask and purged with nitrogen for 30 min, prior to immersion in an oil bath set at 70 °C for 20 h. The resulting copolymer was analysed by DMF GPC (M_n = 28 700 g mol^{-1}, M_w/M_n = 1.25 *vs.* PMMA standards). ^{1}H NMR spectroscopy analysis of the freeze-dried copolymer redissolved in d_7-DMF indicated less than 1% residual BzMA monomer. DLS studies of a 0.20% w/w copolymer dispersion indicated an intensity-average particle diameter of 67 nm (DLS polydispersity = 0.08).

RAFT seeded emulsion polymerisation of linear G_{37}–H_{60}–B_{30} worms

G_{37} macro-CTA (1.00 g, 0.16 mmol), HPMA monomer (1.41 g, 9.76 mmol), ACVA (9.11 mg, 0.033 mmol, CTA/ACVA molar ratio = 5.0) and previously degassed deionised water (21.75 g, 10% w/w), were weighed into a 50 mL round-bottomed flask. The reaction solution was purged with N_2 for 30 min prior to immersion in an oil bath set at 70 °C. The reaction solution was stirred for 2 h at this temperature under a N_2 atmosphere prior to the addition of BzMA (0.86 g, 0.616 mmol). The colloidal dispersion was stirred for a further 4 h to ensure complete BzMA monomer conversion and the polymerisation was quenched by exposure to air.

Preparation of Pickering emulsions and colloidosomes

Either *n*-dodecane or *n*-hexane (2.0 mL) was homogenised with 2.0 mL of a 0.05–2.00% w/w aqueous copolymer dispersion for 2 min at 20 °C using a IKA Ultra-Turrax T-18 homogeniser with a 10 mm dispersing tool operating at 12 000 rpm. All emulsions proved to be stable with respect to droplet coalescence for months on standing at 20 °C. To prepare the colloidosomes, PPG-TDI (8.0 mg) crosslinker was weighed into a sample vial and then dissolved in *n*-hexane (2.0 mL) prior to homogenisation with the aqueous copolymer dispersion. The resulting stable milky-white emulsion was allowed to stand at 20 °C for 1 h to allow urethane bond formation between the terminal isocyanate groups on the cross-linker and the hydroxyl groups on the PGMA (and/or PHPMA) chains.

DMF GPC

Molecular weights and polydispersities were assessed using a gel permeation chromatography (GPC) instrument equipped with a Varian 290-LC pump injection module, a Varian 390-LC refractive index detector, two Polymer Laboratories PL gel 5 μm Mixed-C columns with a DMF mobile phase containing 0.01 M LiBr operating at 60 °C with a constant flow rate of 1.0 mL min^{-1}. DMSO was used as a flow rate marker and calibration was achieved using a series of near-monodisperse poly(methyl methacrylate) standards.

^{1}H NMR spectroscopy

^{1}H NMR spectra were recorded in either D_2O or CD_3OD using a Bruker Avance 400 spectrometer operating at 400 MHz.

Dynamic light scattering (DLS)

Intensity-average hydrodynamic diameters were obtained by DLS using a Malvern Zetasizer NanoZS instrument at a fixed scattering angle of 173°. Aqueous dispersions of 0.01% w/w particles were analysed using disposable cuvettes and the results were averaged over three consecutive runs. The deionised water used to dilute each sample was ultra-filtered through a 0.20 μm membrane in order to remove extraneous dust.

Transmission electron microscopy

Aqueous particle dispersions were diluted fifty-fold at 20 °C to generate 0.20% w/w dispersions for transmission electron microscopy (TEM) studies. Copper/palladium TEM grids (Agar Scientific) were surface-coated in-house to produce a thin film of amorphous carbon. The grids were then plasma glow-discharged for 30 seconds to create a hydrophilic surface. Individual samples (0.20% w/w, 12 μL) were adsorbed onto the freshly glow-discharged grids for one minute and then blotted with filter paper to remove excess solution. To stain the copolymer aggregates, uranyl formate solution (0.75% w/w; 9 μL) was soaked on the sample-loaded grid for 20 seconds and then carefully blotted to remove excess stain. The grids were then dried using a vacuum hose. Imaging was performed at 100 kV using a Phillips CM100 instrument equipped with a Gatan 1 k CCD camera.

Optical microscopy

Optical microscopy images of Pickering emulsion droplets were recorded using a Motic DMBA300 digital biological microscope equipped with a built-in camera and analysed using Motic Images Plus 2.0 ML software.

Laser diffraction

Each emulsion was sized using a Malvern Mastersizer 2000 instrument equipped with a small volume Hydro 2000SM sample dispersion unit (*ca.* 50 mL), a HeNe laser operating at 633 nm and a solid-state blue laser operating at 466 nm. The stirring rate was adjusted to 1000 rpm in order to avoid creaming of the emulsion during analysis. After each

measurement, the cell was rinsed once with ethanol, followed by three rinses with doubly-distilled water; the glass walls of the cell were carefully wiped with lens cleaning tissue to avoid cross-contamination and the laser was aligned centrally to the detector prior to data acquisition.

Determination of Pickering emulsifier efficiency *via* either turbidimetry or UV spectroscopy

The nanoparticle adsorption efficiency at the oil–water interface was determined by analysis of the lower aqueous phase after creaming of the oil droplets had occurred on standing. The remaining non-adsorbed nanoparticles were detected and thus the fraction of adsorbed nanoparticles was calculated indirectly by difference. Turbidimetry was used for the crosslinked G_x–H_y–E_z nanoparticles, with scattering curves being determined for known concentrations of aqueous copolymer dispersions in order to produce a linear calibration plot of absorbance *versus* concentration at an arbitrary wavelength of 750 nm (see ESI, Fig. S3†). For the linear PBzMA-based nanoparticles (G_{51}–B_{250} and G_{37}–H_{60}–B_{30}), calibration plots were constructed in DMF, which leads to molecular dissolution of the copolymer chains. The UV absorbance at 269 nm assigned to the aromatic benzyl groups on the PBzMA blocks was determined as a function of copolymer concentration to obtain a linear calibration plot (see ESI, Fig. S3†). The lower aqueous phases of these creamed Pickering emulsions were then dried at 50 °C for 120 h prior to molecular dissolution of the copolymer in DMF. [This protocol was essential to avoid UV scattering problems, but it could not be utilised for the crosslinked worms described above since these nanoparticles cannot be molecularly dissolved.] The fraction of nanoparticles adsorbed onto the oil droplets was then calculated by difference.

Results and discussion

The synthetic route used to prepare Pickering emulsions and colloidosomes using either spherical or worm-like PGMA–PHPMA nanoparticles is shown in Fig. 1. We have previously reported that the analogous block copolymer vesicles can stabilise *n*-dodecane emulsions.[32] However, it was found that an EGDMA cross-linker was essential to retain the vesicular morphology during high shear homogenisation in order to obtain genuine Pickering emulsions. In contrast, linear vesicles prepared in the absence of any EGDMA did not survive the high-shear emulsification conditions. Instead, vesicular dissociation occurred to produce individual copolymer chains which subsequently acted as macromolecular surfactants for the emulsion droplets.

In the present work, we wished to investigate whether the problem of shear-induced particle disintegration was restricted to vesicles or also applied to spherical nanoparticles and worm-like micelles. It has been previously shown that *linear* PGMA–PHPMA vesicles are relatively delicate: they undergo partial collapse under ultrahigh vacuum conditions[27] and do not tolerate the addition of ionic surfactants.[33] Thus it was conceivable that the vesicular copolymer morphology alone was

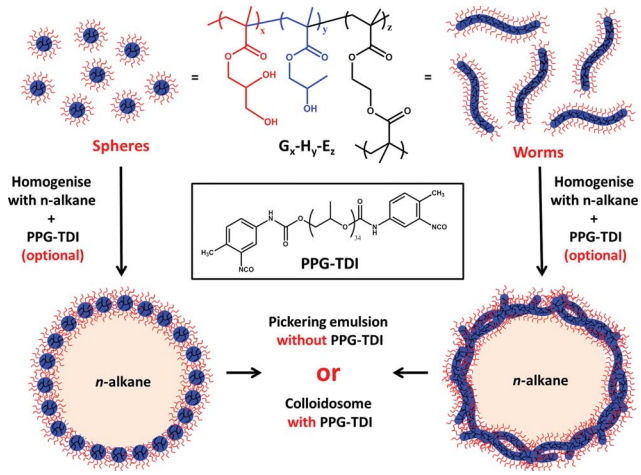

Fig. 1 Synthetic route to Pickering emulsions using (left) spherical or (right) worm-like triblock copolymer nanoparticles prepared by RAFT aqueous dispersion polymerisation of HPMA at 70 °C using a PGMA macro-CTA stabiliser and an EGDMA cross-linker. The relative mean degrees of polymerisation of the PGMA and PHPMA blocks (*x* or *y*, respectively) dictate their relative volume fractions and hence the final nanoparticle morphology. Colloidosomes are obtained simply by addition of PPG-TDI cross-linker to the oil phase prior to homogenisation, which was conducted at 12 000 rpm for 2 min at 20 °C.

the primary reason for the disintegration observed during high-shear emulsification. On the other hand, it is also known that the PHPMA block is only weakly hydrophobic. For example, variable temperature ^{1}H NMR studies indicate that significant plasticisation of the core-forming PHPMA block occurs on cooling an aqueous dispersion of PGMA–PHPMA worms from 25 °C to 5 °C, which is sufficient to induce a worm-to-sphere order–order transition.[34] Thus the specific block composition (rather than the vesicular morphology *per se*) could be the main reason for the vesicle dissociation observed in the absence of chemical cross-linker. If this were the case, then linear PGMA–PHPMA spheres and worms might also be expected to break up when subjected to the same high shear conditions.

In order to further investigate the possible loss of copolymer morphology during high shear emulsification, six examples of linear and crosslinked block copolymer worms and spheres were prepared using RAFT-mediated PISA formulations. Table 1 summarises the copolymer morphologies, molecular weight data and DLS diameters obtained for the various G–H, G–H–E, G–Bz and G–H–B nanoparticles used in this investigation. It is emphasised that DLS reports a *spherical-average* hydrodynamic diameter based on the Stokes–Einstein equation; thus this parameter should be treated with some caution when considering highly anisotropic worm-like particles.

Representative TEM images obtained for the six types of block copolymer nanoparticles summarised in Table 1 are shown in Fig. 2. The synthesis of crosslinked spherical nanoparticles (G_{100}–H_{200}–E_{20}) was relatively straightforward, with 10 mol% EGDMA (based on HPMA monomer) simply being added at the end of the HPMA polymerisation.[23] In this case, the cross-linker has minimal effect on both the particle size and

Table 1 Target block compositions, copolymer morphologies, molecular weight data and DLS hydrodynamic diameters for the six types of block copolymer nanoparticles evaluated in this work for the preparation of Pickering emulsions and colloidosomes

Target block copolymer composition	Copolymer morphology	Linear or crosslinked?	M_n[b]/ g mol^{-1}	M_w/M_n	DLS diameter (PDI)/nm	Average worm contour length (nm)	Droplet diameter at 0.06% w/w (μm)	Pickering adsorption efficiency[a] (%)	Droplet surface coverage at maximum efficiency[a]
G_{100}–H_{200}	Spheres	Linear	82 800	1.20	50 (0.14)	—	48 ± 14	—	—
G_{100}–H_{200}–E_{20}	Spheres	Crosslinked	—	—	47 (0.13)	—	237 ± 129	90	0.93
G_{45}–H_{140}	Worms	Linear	39 300	1.08	315 (0.34)	176 ± 115	46 ± 14	—	—
G_{45}–H_{100}–E_{10}	Worms	Crosslinked	—	—	122 (0.28)	172 ± 117	179 ± 50	90	0.47
G_{51}–B_{250}	Spheres	Linear	51 100	1.19	81 (0.10)	—	418 ± 117	80	0.91
G_{37}–H_{60}–B_{30}	Worms	Linear	21000	1.16	72 (0.21)	120 ± 90	219 ± 73	100	0.71

[a] Calculated at 0.06% w/w copolymer concentration.

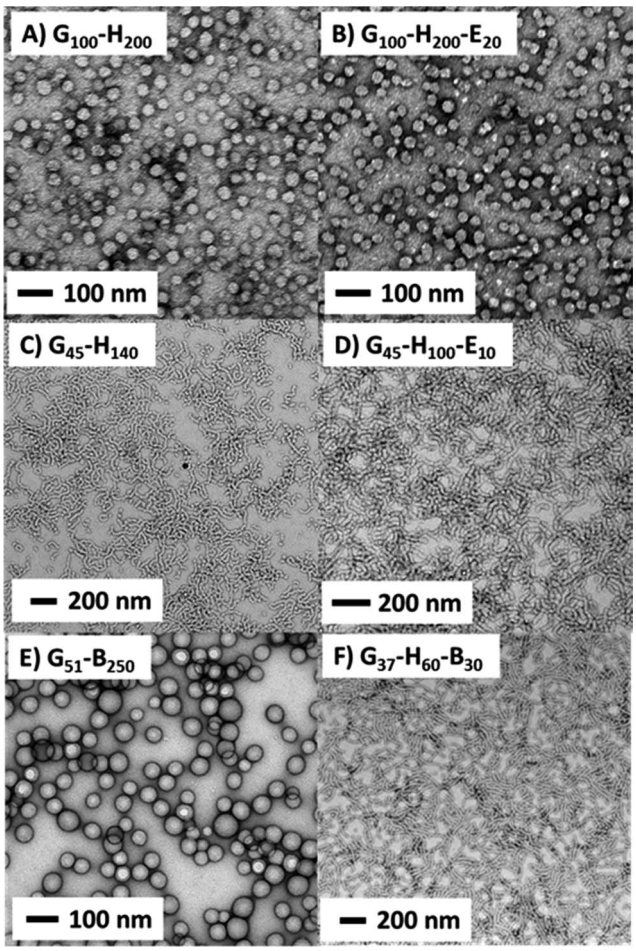

Fig. 2 Representative transmission electron microscopy images obtained for: (A) linear G_{100}–H_{200} spherical nanoparticles, (B) crosslinked G_{100}–H_{200}–E_{20} spherical nanoparticles, (C) linear G_{45}–H_{140} worms, (D) crosslinked G_{45}–H_{100}–E_{10} worms, (E) linear G_{51}–B_{250} spheres and (F) linear G_{37}–H_{60}–B_{30} worms.

morphology, with uniform spheres of around 50 nm diameter being produced both in the presence and absence of EGDMA. In contrast, the preparation of crosslinked worms was rather more problematic. This is presumably because the pure worm phase occupies a relatively narrow region of the phase diagram.[27] Highly anisotropic flexible worms were obtained when targeting a G_{45}–H_{140} diblock (see Fig. 2C). However, replacing 10 units of HPMA with the same number of EGDMA units (*i.e.* targeting G_{45}–H_{130}–E_{10}) only resulted in a mixed vesicle/worm phase (see Fig. S1 in the ESI†). It seems that the addition of cross-linker shifts the vesicle/worm phase boundary, at least for this particular formulation. In view of this problem, a shorter PHPMA block was targeted to afford an overall triblock composition of G_{45}–H_{100}–E_{10}. Fortunately, this formulation yielded a pure phase comprising crosslinked worms (Fig. 2D). Recently, we have found that RAFT aqueous emulsion polymerisation of BzMA using a PGMA macro-CTA invariably gives a purely spherical morphology, regardless of the target block DPs or copolymer concentration.[35] This also proved to be the case in the present work, with G_{51}–B_{250} forming well-defined, near-monodisperse spherical nanoparticles with a DLS diameter of 67 nm. In striking contrast, growing a relatively short PHPMA block from the PGMA macro-CTA prior to BzMA polymerisation leads to well-defined worms when targeting a G_{37}–H_{60}–B_{30} composition. This particular triblock copolymer formulation is perhaps best considered as an example of a RAFT aqueous emulsion polymerisation of BzMA using a G_{37}–H_{60} diblock copolymer precursor. DLS analysis of this precursor indicates the presence of ill-defined, weakly scattering nano-objects with a sphere-equivalent diameter of 141 nm. This suggests that this diblock precursor has not actually undergone micellar nucleation prior to BzMA addition and is therefore likely to comprise weakly interacting molecularly-dissolved copolymer chains. This unusual RAFT PISA formulation clearly warrants further work, but in the present study it is simply exploited as a convenient route to linear G_{37}–H_{60}–B_{30} worms that comprise a strongly hydrophobic PBzMA block in addition to the weakly hydrophobic PHPMA block.

Previously, Blanazs *et al.* reported that G_{54}–H_{140} linear worms exhibit thermo-responsive behaviour in aqueous solution at 10% w/w solids, undergoing a reversible morphological transition to form spheres on cooling from 25 °C to 5 °C as judged by TEM, SAXS and rheology studies.[34] Variable temperature DLS studies confirmed that the G_{45}–H_{140} linear worms

prepared in this work undergo a similar thermal transition (see Fig. 3A). Thus the apparent spherical-average hydrodynamic diameter decreases from 315 nm at 25 °C to just 25 nm at 4 °C, with a concomitant reduction in scattered light from approximately 3×10^5 to 6×10^3 kilocounts per second (kcps). These observations are fully consistent with the worm-to-sphere thermal transition reported previously.[34] Interestingly, further cooling from 4 to 2 °C led to a further reduction in size from 25 nm to 12 nm and a further drop in count rate to 1×10^3 kcps, which suggests further disintegration of the spherical nanoparticles to give either molecularly dissolved or very weakly interacting copolymer chains. A similar second transition has been inferred for a G_{49}–H_{130} diblock copolymer by Kocik *et al.* on the basis of small-angle X-ray scattering studies.[36] Moreover, it is worth emphasising that the corresponding sphere-to-worm transition does not occur on returning to 25 °C for this 0.25% w/w aqueous copolymer solution. Such *irreversible* behaviour is presumably observed because the highly cooperative 1D fusion of multiple spheres to form worms becomes infinitely slow at such high dilution. In contrast, the dissociation of worms to give spheres is not a cooperative process, so it is relatively unaffected at such low copolymer concentrations. Fig. S2† indicates that copolymer concentrations of at least 1.0% w/w are required for the linear G_{45}–H_{145} worms to regain their original sphere-equivalent diameter after a cooling/warming cycle.

In contrast, the crosslinked G_{45}–H_{100}–E_{10} worms exhibit qualitatively different behaviour on cooling a 0.25% w/w aqueous dispersion from 25 °C to 5 °C, see Fig. 3B. There is essentially no change in the apparent sphere-equivalent diameter on either cooling or heating, indicating that no worm-to-sphere transition occurs in this case. These negative observations are of course fully consistent with the additional covalent stabilisation conferred by the EGDMA cross-linker. Similarly, there is no discernible change in particle size during the same thermal cycle for the G_{37}–H_{60}–B_{30} worms. Thus it appears that the PBzMA block is sufficiently hydrophobic to suppress the thermo-responsive nature of the PHPMA block, with the former conferring additional physical stabilisation *via* enhanced hydrophobic interactions between the core-forming blocks. In principle, the greater stability indicated by the lack of thermal response observed for the chemically or physically crosslinked worms is likely to enhance the ability of such nanoparticles to survive high-shear emulsification (see later).

Initially, the linear G_{100}–H_{200} and crosslinked G_{100}–H_{200}–E_{20} spherical nanoparticles were compared as putative Pickering emulsifiers.

Fig. 4 shows how the mean droplet diameter varies with copolymer concentration for these two dispersions. For the chemically crosslinked G_{100}–H_{200}–E_{20} nanoparticles, smaller oil

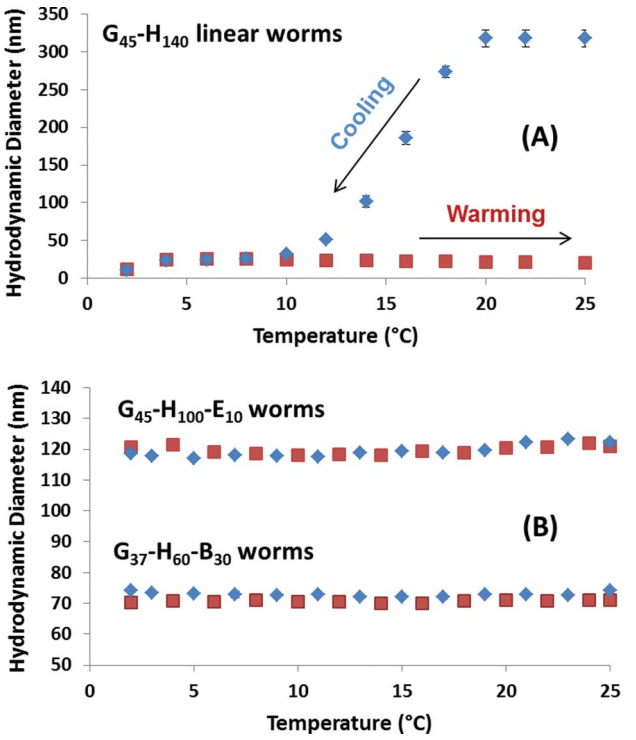

Fig. 3 Variable temperature DLS studies obtained for 0.25% w/w aqueous dispersions of linear (A) G_{45}–H_{140} worms, and (B) crosslinked G_{45}–H_{100}–E_{10} worms and linear G_{37}–H_{60}–B_{30} worms (see Table 1). The blue and red data points indicate the change in sphere-equivalent diameter on cooling and heating, respectively. Note the *irreversible* thermo-responsive behaviour observed for the linear G_{45}–H_{140} worms at this relatively low copolymer concentration, and also the lack of any thermo-responsive behaviour found for the other two types of worms. Error bars represent the standard deviation determined for three separate measurements.

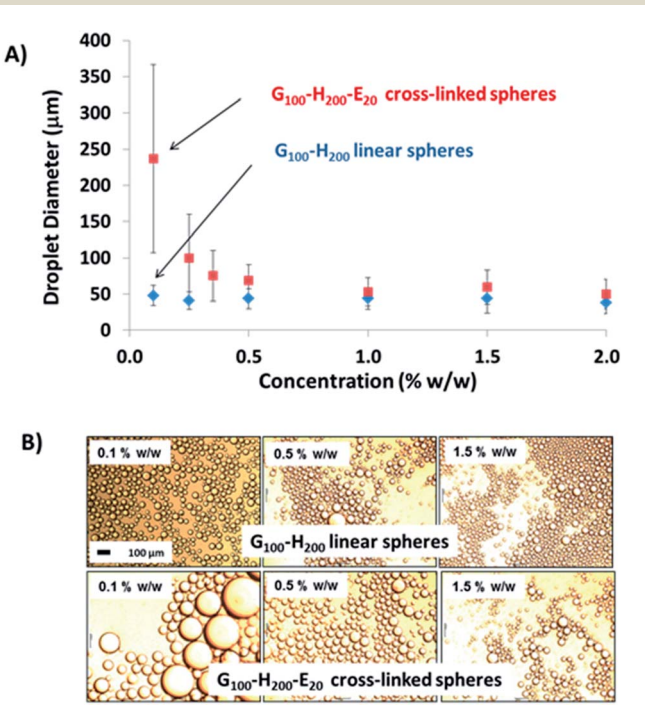

Fig. 4 (A) Mean laser diffraction droplet diameter *versus* copolymer concentration for both linear G_{100}–H_{200} spheres and crosslinked G_{100}–H_{200}–E_{20} spheres. The error bars represent the standard deviation of each mean volume-average droplet diameter, rather than the experimental error. (B) Optical microscopy images recorded for selected emulsions corresponding to the data points shown in (A). The 100 µm scale bar in the first image applies to all images.

droplets are obtained at higher copolymer concentrations. This is because there are more nanoparticles available to coat (and hence) stabilise the oil droplet surface. A minimum mean droplet diameter of approximately 50 μm is obtained at between 0.5 and 1.0% w/w copolymer concentration, which corresponds to the optimum conditions required for emulsification (*i.e.* minimum droplet diameter and maximum adsorption efficiency). This behaviour is typical of a Pickering emulsifier and has been reported for both PGMA-stabilised polystyrene latexes prepared by conventional aqueous emulsion polymerisation[37] and also for the crosslinked G_{53}–H_{350}–E_{20} vesicles discussed earlier.[32] The maximum adsorption efficiency for these G_{100}–H_{200}–E_{20} spheres was calculated to be 90% based on turbidimetry studies of the lower aqueous phase of the emulsion after creaming of the oil droplets. This makes them rather more efficient than the previously reported crosslinked G_{53}–H_{350}–E_{20} vesicles,[32] but less efficient than the (larger) $PGMA_{50}$–PS latex particles.[37]

In contrast, no significant change in the mean oil droplet diameter occurs when varying the concentration of the *linear* G_{100}–H_{200} spherical nanoparticles. Taken at face value, these data suggest that the linear spheres can stabilise smaller oil droplets than the crosslinked spheres at a given copolymer concentration (<1.0% w/w). Given that these nanoparticles are essentially the same size, this should not be the case if they adsorb with similar packing densities at the surface of the oil droplets. In principle, the surface coverage (C_s) for these spherical nanoparticles packed around large spherical oil droplets can be calculated using eqn (1) below, as reported previously.[11]

$$C_s = \frac{m_p D}{4\rho_p d_p V_d} \quad (1)$$

This equation is simply the surface area of the adsorbed particles divided by the surface area of the droplets, where C_s is the surface coverage of the droplets by the spherical nanoparticles, D is the mean droplet diameter (as determined by laser diffraction), m_p is the mean nanoparticle mass, ρ_p is the nanoparticle density, d_p is the mean nanoparticle radius (as determined by DLS) and V_d is the total volume of the oil droplet phase. In the case of the crosslinked G_{100}–H_{200}–E_{20} nanoparticles of 47 nm diameter, oil droplets with a mean diameter of 237 μm are produced at a copolymer concentration of 0.10% w/w (assuming an adsorption efficiency of 90%, see Table 1). This suggests a C_s value of approximately 0.93, indicating that the entire oil droplet surface is uniformly coated with close-packed nanoparticles. This is certainly consistent with a stable emulsion, since such a dense nanoparticle layer should prevent droplet coalescence. Indeed, TEM provides good evidence for a close-packed monolayer of spherical nanoparticles for this particular system (see later). In principle, P should not exceed 0.84 for small monodisperse spheres packed as a monolayer on larger spheres.[38] In practice, this modest discrepancy simply reflects the various approximations that are inherent in such calculations.

In the case of the *linear* G_{100}–H_{200} spherical nanoparticles, the same 0.10% w/w copolymer concentration affords stable oil droplets of approximately 48 μm diameter. Using eqn (1), we calculate $C_s = 0.19$ under these conditions, which suggests that only 19% of the droplet surface is coated by the nanoparticles. Given an oil volume fraction of 0.50, this C_s value seems to be rather low to account for the excellent long-term droplet stability that is observed experimentally, particularly given that the almost identical crosslinked G_{100}–H_{200}–E_{20} nanoparticles exhibit such a comparatively high surface coverage. Instead, a more likely scenario is that these oil droplets are actually stabilised by *individual* G_{100}–H_{200} copolymer chains, which are generated *via* dissociation of the linear G_{100}–H_{200} spherical nanoparticles during high shear homogenisation. Thus, as found for the crosslinked G_{53}–H_{350}–E_{20} vesicles discussed earlier,[32] the EGDMA comonomer is essential to preserve the original copolymer morphology generated during the PISA synthesis and hence ensure that a true Pickering emulsion is obtained (as opposed to emulsion droplets stabilised by a molecularly-dissolved G_{100}–H_{200} diblock copolymer surfactant).

The same experiments were performed on the linear G_{45}–H_{140} and crosslinked G_{45}–H_{100}–E_{10} worms, see Fig. 5. An aqueous dispersion of the linear worms was diluted immediately prior to emulsion preparation at 20 °C in order to avoid inadvertently triggering the worm-to-sphere transition. Thus such nanoparticles should be present in their original worm morphology (and this was confirmed by TEM studies). As a comparison, emulsions were also prepared by conducting high-shear homogenisation at 0 °C with the aid of an ice bath. The crosslinked worms displayed similar behaviour to the crosslinked spherical nanoparticles discussed above, and also the crosslinked vesicles reported previously.[32] The mean size of the oil droplets is gradually reduced at higher copolymer concentrations until a limiting minimum diameter of around 49 μm is attained. The maximum adsorption efficiency is again approximately 90%, making the affinity of these crosslinked worms for the *n*-dodecane–water surface comparable to that of the crosslinked spheres. This is perfectly reasonable given that they are both G_x–H_y–E_z copolymers, which should hence exhibit similar particle wettabilities at the oil–water interface. However, it is worth emphasising that, although the same Pickering adsorption efficiency (90%) is observed in both cases, the worms produce significantly smaller oil droplets at approximately half the surface coverage (0.47 *vs.* 0.93; see Table 1). For example, when using an initial copolymer concentration of 0.10% w/w (for which the final supernatant concentration of non-adsorbed copolymer is ~0.01% w/w in both cases), the mean droplet diameter is 237 μm for the crosslinked spheres, but only 131 μm for the crosslinked worms. Hence the total surface area of the latter oil droplets is significantly higher. This is because the high aspect ratio of the worms allows the droplet surface to become sufficiently coated to prevent coalescence at a somewhat lower packing fraction than that of the spherical particles, particularly when working at such low copolymer concentrations. It is hypothesised that the nanoparticle packing fraction on the oil droplet surface gradually increases when using higher

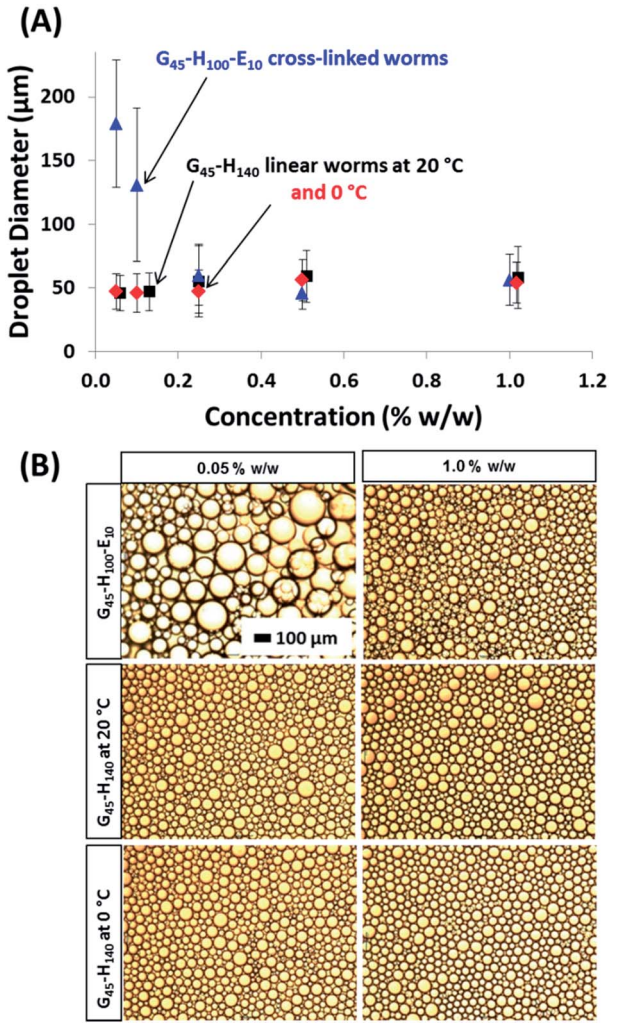

Fig. 5 (A) Mean laser diffraction droplet diameter *versus* copolymer concentration for both linear G_{45}–H_{140} and crosslinked G_{45}–H_{100}–E_{10} worms. The corresponding data obtained for the linear G_{45}–H_{140} worms utilised for high-shear homogenisation conducted at 0 °C is also shown. The error bars represent the standard deviation of each mean volume-average droplet diameter, rather than the experimental error. (B) Optical microscopy images for selected emulsions corresponding to data points shown in (A). The 100 μm scale bar shown in the top left image applies to all six images.

concentrations of the crosslinked worms, instead of remaining essentially constant as found for the spherical nanoparticles.

Using the linear worms produced oil droplet diameters of approximately 50 μm, regardless of the copolymer concentration. This indicates that the linear worm morphology is not sufficiently robust to survive the high-shear homogenisation conditions, thus the oil droplets formed in this case are actually stabilised by individual copolymer chains. This interpretation is supported by the data obtained using the linear worms for emulsifications conducted at around 0 °C. Under these conditions, DLS studies suggest that linear worms dissociate to produce essentially molecularly-dissolved copolymer chains, see Fig. 3. Hence this is consistent with the almost identical droplet diameter *vs.* copolymer concentration data sets obtained when using the linear worms at 25 °C and 0 °C, see Fig. 5A.

PGMA-stabilised polystyrene latex particles have been previously employed by Thompson *et al.* for the preparation of covalently crosslinked colloidosome microcapsules.[37] The hydroxyl groups on the PGMA steric stabiliser chains are readily amenable to crosslinking using an oil-soluble polymeric diisocyanate (PPG-TDI), which leads to the formation of colloidosomes. Importantly, these covalently-stabilised latex superstructures can survive an ethanol challenge intact, even after complete removal of the oil droplet phase. In the present work, we used the same approach to cross-link the various linear and crosslinked PGMA–PHPMA nanoparticles (or linear copolymer chains) at the oil–water interface in order to study the copolymer morphology *via* TEM. However, ethanol is a good solvent for the core-forming PHPMA block and is thus likely to swell or even dissolve the copolymer nanoparticles. Therefore an alternative approach was required: *n*-hexane was employed instead of *n*-dodecane to allow convenient removal of the oil phase *via* evaporation, rather than *via* an ethanol challenge. The PPG-TDI crosslinker was dissolved in *n*-hexane prior to homogenisation and the resulting emulsion was allowed to stand at 20 °C for 1 h to enable cross-linking to occur. The *n*-hexane was then evaporated by magnetically stirring the diluted aqueous colloidosome suspension exposed to the atmosphere at 20 °C (at the back of a fume hood). Intact microcapsules were observed by optical microscopy for both worms and spheres prepared either with or without the EGDMA crosslinker. These microcapsules were imaged by TEM to assess the copolymer morphology. Fig. 6 shows the microcapsules prepared using the linear G_{100}–H_{200} spheres and the linear G_{45}–H_{140} worms. The microcapsule surface is completely smooth and featureless in each case, with no evidence for any adsorbed copolymer particles. Thus the microcapsule shell appears to comprise a *molecular film* of PPG-TDI crosslinked PGMA–PHPMA copolymer chains. These observations are fully consistent with the concentration-independent droplet diameters observed when employing such linear nanoparticles as putative Pickering emulsifiers. Moreover, similar TEM observations were reported for linear $PGMA_x$–$PHPMA_y$ vesicles in our earlier study.[32] Thus all the experimental evidence suggests that linear PGMA–PHPMA nanoparticles are not sufficiently robust to survive high shear homogenisation.

In contrast, Fig. 6C and D shows TEM images obtained for colloidosomes prepared using crosslinked G_{100}–H_{200}–E_{20} spherical nanoparticles and crosslinked G_{45}–H_{100}–E_{10} worms, respectively. Clearly, the former emulsifier leads to the formation of colloidosomes that comprise densely-packed spherical nanoparticles. This image is consistent with the high packing efficiency calculated above, but is in striking contrast to the smooth, featureless microcapsule surface obtained when using the corresponding *linear* spherical nanoparticles. Moreover, it is perhaps worth noting that the inter-particle separation distance within the colloidosome wall is significantly smaller than in our previous work,[37] which in principle could lead to enhanced retention of macromolecules or nanoparticles encapsulated within such colloidosomes.[39]

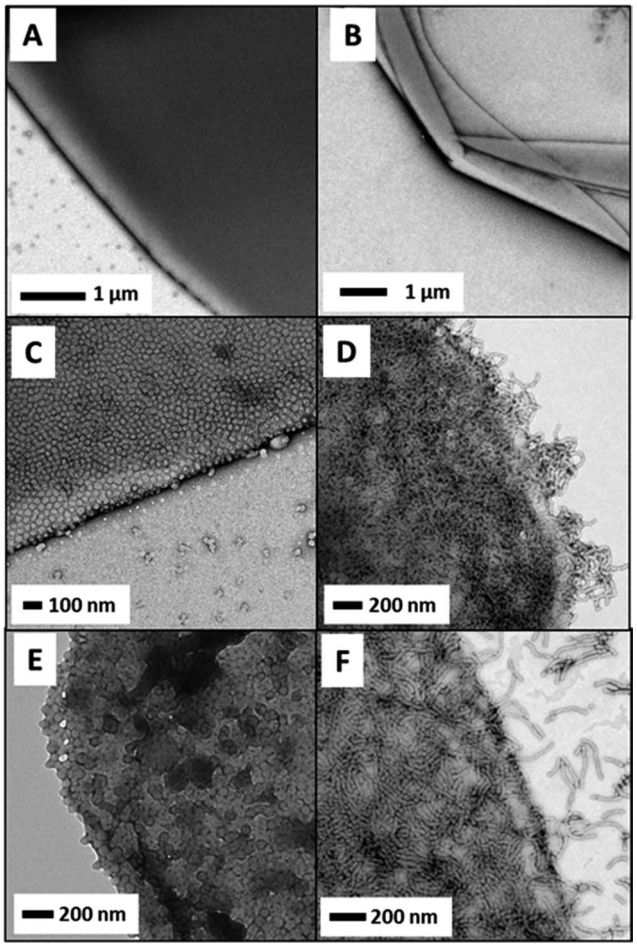

Fig. 6 TEM images of the edge and surface of various microcapsules prepared at 20 °C using: (A) linear G_{100}–H_{200} spheres, (B) linear G_{45}–H_{145} worms, (C) crosslinked G_{100}–H_{200}–E_{20} spheres, (D) crosslinked G_{45}–H_{100}–E_{10} worms, (E) linear G_{51}–B_{250} spheres and (F) linear G_{37}–H_{60}–B_{30} worms. Note the smooth, featureless surface with no indication of any adsorbed nanoparticles in both (A) and (B). This suggests that these linear nanoparticles have each dissociated during high shear homogenisation and are actually present as adsorbed copolymer chains, rather than as nanoparticles. In contrast, the morphology of the original nanoparticles is clearly visible in images (C) to (F). [N.B. images (A) to (E) were obtained for PPG-TDI crosslinked colloidosomes, whereas image (F) was obtained for a dried Pickering emulsion droplet.]

A densely-packed layer of nanoparticles is also observed on the surface of colloidosomes prepared using the crosslinked G_{45}–H_{100}–E_{10} worms (see Fig. 6D). In the literature, it is generally assumed that highly anisotropic *rod-like* particles such as ellipsoidal polystyrene particles lie predominately flat at both the oil–water and air–water interfaces.[16,40,41] Similar behaviour is also observed for cellulose nanofibers.[18,19] In the present study, this also seems to be the case for the majority of worms, although some worms do appear to protrude out from the edge of the colloidosome surface. However, it is not clear whether this is actually the case in the 'wet' emulsion, or if this is simply a drying artefact that arises during TEM grid preparation. In principle, it may be feasible for some fraction of a relatively long worm to become adsorbed within the plane of the droplet surface, with the remainder of the worm extending out into the aqueous phase. Given the relatively flexible nature of these worms, this hypothesis is not unreasonable (particularly in the limit of high worm coverage).

Overall, it is clear that linear PGMA–PHPMA diblock copolymers in the form of either spherical nanoparticles or worms dissociate during homogenisation (just like the analogous vesicles reported earlier[32]) to produce individual copolymer chains. Under such high-shear emulsification conditions, the EGDMA cross-linker is essential to preserve the original copolymer morphology and hence ensure genuine Pickering stabilisation of the oil droplets, as opposed to emulsion stabilisation *via* molecularly-dissolved block copolymer surfactant. However, PHPMA is known to be only weakly hydrophobic,[42] so we decided to examine whether a more hydrophobic core-forming block could enhance the stability of such nano-objects when evaluated as putative Pickering emulsifiers.

To address this important question, linear G_{51}–B_{200} spherical nanoparticles of approximately 67 nm diameter were prepared *via* RAFT aqueous emulsion polymerisation for assessment as a Pickering emulsifier. Accordingly, these nanoparticles were homogenised with *n*-dodecane at various copolymer concentrations and the resulting emulsions were characterised using optical microscopy and laser diffraction (see Fig. 7).[43] Using the G_{51}–B_{200} spheres leads to a strongly concentration-dependent droplet diameter, unlike the earlier data set obtained for the linear G_{100}–H_{200} spherical

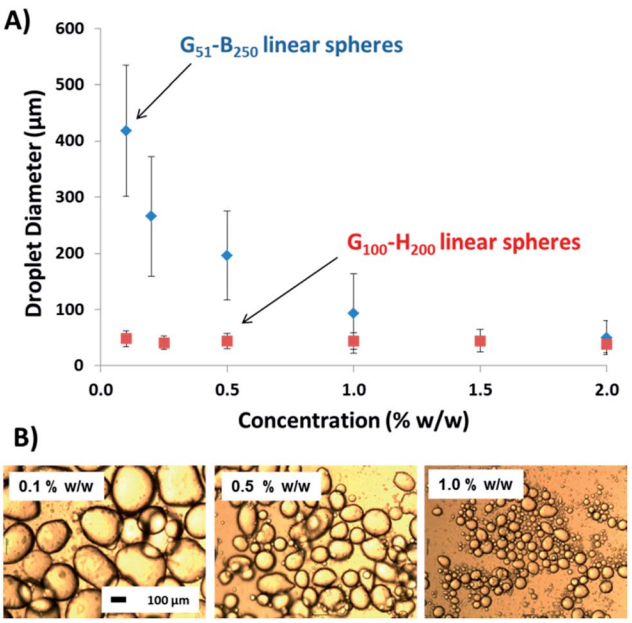

Fig. 7 (A) Laser diffraction volume-average droplet diameter against copolymer concentration for G_{51}–B_{250} spheres and G_{100}–H_{200} linear spheres for comparison. The error bars represent the standard deviation of the mean droplet diameter, rather than the experimental error. (B) Optical microscopy images obtained for selected emulsions stabilised using the G_{51}–B_{250} spheres. The 100 μm scale bar shown in the left-hand image applies to all three images.

nanoparticles (which is included in Fig. 7 to aid direct comparison). The increase in mean droplet diameter observed on lowering the concentration of the linear G_{51}–B_{250} spheres is fully consistent with the behaviour of the EGDMA crosslinked nanoparticles discussed above, as well as the PGMA–PS latexes reported earlier.[37] TEM imaging of the colloidosome surface prepared with these G_{51}–B_{250} spheres also shows fully intact spheres adsorbed at the droplet interface. Thus it appears that chemical cross-linking is not a pre-requisite to preserve the original copolymer morphology during homogenisation provided that the core-forming block is sufficiently hydrophobic to stabilise the nanoparticles with respect to their shear-induced dissociation.

Finally, high shear emulsification of *n*-dodecane was conducted in the presence of the linear G_{37}–H_{60}–B_{30} worms. The important question here is: does a relatively short PBzMA block confer sufficient stability to the worms so as to enable the formation of a genuine Pickering emulsion? Fig. 8 confirms that larger droplets are formed as the worm concentration is gradually reduced. In view of the data sets discussed above, this strongly suggests that these anisotropic nanoparticles adsorb intact at the oil–water interface, in contrast to the molecularly-dissolved copolymer chains obtained when examining the linear G_{45}–H_{140} worms. As indicated by the absence of a worm-to-sphere transition for G_{37}–H_{60}–B_{30} (see Fig. 3), even a relatively short PBzMA block is sufficient to stabilise these worms during high-shear emulsification; in this case nanoparticle dissociation is prevented as a result of the significantly stronger hydrophobic interactions between the core-forming blocks. This is further confirmed by TEM analysis of the colloidosome surface in Fig. 6F, which clearly shows that the original worm-like morphology is preserved at the droplet surface. It is also emphasised that these G_{37}–H_{60}–B_{30} worms proved to be extremely efficient Pickering emulsifiers: no worms could be detected in the supernatant phase after droplet creaming, suggesting essentially 100% adsorption at the oil–water interface. We speculate that this enhanced efficiency compared to the EGDMA crosslinked worms may be a result of the more hydrophobic PBzMA block increasing the particle contact angle at the oil–water interface, hence leading to stronger adsorption.

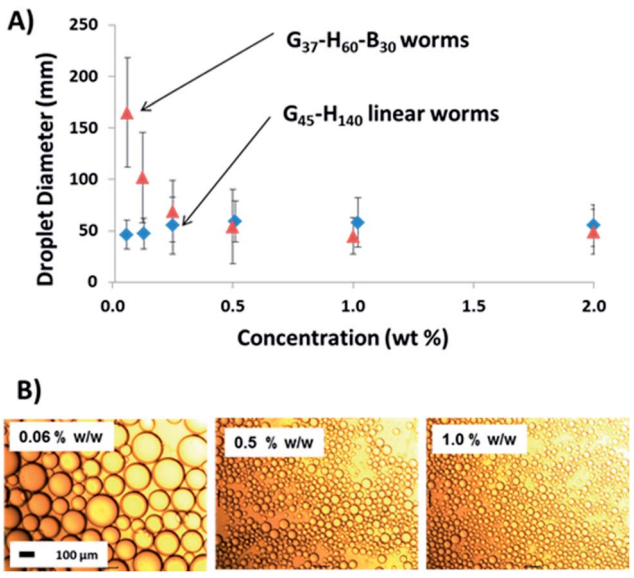

Fig. 8 (A) Laser diffraction volume-average droplet diameter against copolymer concentration for two sets of linear worms (G_{37}–H_{60}–B_{30} and G_{45}–H_{140}). Only the former worms act as a genuine Pickering emulsifier; the latter worms undergo molecular dissolution during high shear emulsification and instead act as a block copolymer surfactant. The error bars represent the standard deviation of the mean droplet diameter, rather than the experimental error. (B) Optical microscopy images obtained for selected emulsions stabilised using the G_{37}–H_{60}–B_{30} linear worms. The 100 μm scale bar applies to all images.

It is worth emphasising that, in general, the worms can be considered to be more effective Pickering emulsifiers than the equivalent spherical nanoparticles. More specifically, they are at least as efficiently (and almost certainly rather more strongly) adsorbed at the droplet interface. Moreover, smaller oil droplets are consistently produced when worms are used as the Pickering emulsifier when compared to an equal mass of spherical nanoparticles. The surface coverage (C_w) of the worms adsorbed on the surface of the oil droplets can be estimated using a modified version of eqn (1), which was derived for spherical nanoparticles.

$$C_w = \frac{m_p D}{6\rho_p h_p V_d} \quad (2)$$

The main difference between eqn (1) and (2) is that h_p now represents the mean worm thickness (estimated from TEM) rather than the sphere diameter. The surface coverages calculated for the lower worm concentrations are shown in Table 1. Worm surface coverages, C_w, of 0.47 and 0.63, are calculated for the EGDMA and BzMA stabilised worms respectively. These values are significantly lower than those obtained for oil droplets stabilised using spherical nanoparticles. The reciprocal of the mean oil droplet diameter, D, is plotted against the mass of adsorbed worms, m_p, in Fig. 9a. According to eqn (2), the gradient should be inversely proportional to the worm surface coverage (C_w).[19,20]

Thus two distinct surface coverage regimes can be obtained, depending on the copolymer concentration used to prepare the Pickering emulsions. Very similar behaviour has been recently reported by Kalashnikova *et al.*[19] for anisotropic Pickering emulsifiers based on bacterial cellulose nanofibres. At a relatively high copolymer concentration (*e.g.* 1.0% w/w) a high surface coverage is obtained, while at a relatively low copolymer concentration (*e.g.* 0.10% w/w) a significantly lower surface coverage is observed. [In contrast, a linear plot – indicating a single 'high surface coverage' regime - is obtained for the crosslinked spheres, see Fig. S4 in the ESI.†] This was confirmed by TEM analysis of dried Pickering emulsion droplets (prepared using *n*-hexane as the oil phase and in the absence of any PPG-TDI crosslinker) for both copolymer concentrations (*i.e.* 0.10 and 1.0% w/w) of the G_{37}–H_{60}–B_{30} triblock copolymer worms (see representative images shown in Fig. 9b and c, respectively). Clearly, the Pickering emulsion droplet surface is much more densely packed with worms when using the higher copolymer

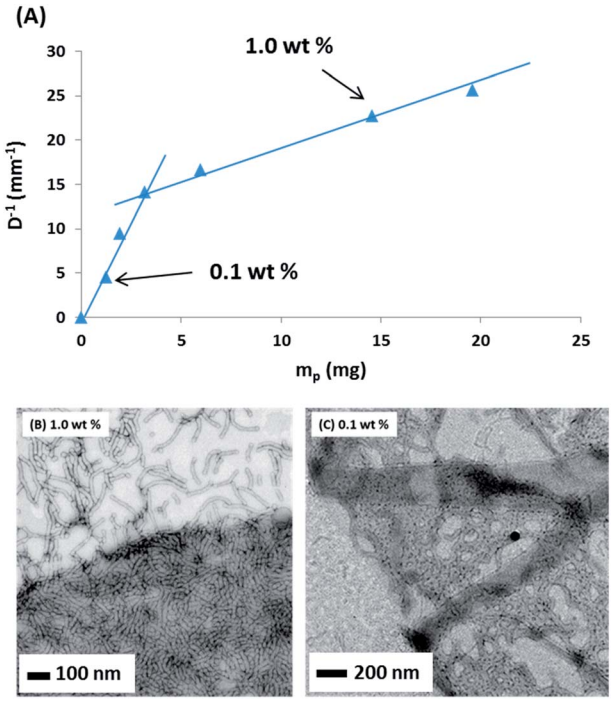

Fig. 9 (A) Variation of the reciprocal of the mean oil droplet diameter (D^{-1}) with nanoparticle mass (m_p) for linear G_{37}–H_{60}–B_{30} worms (top). The gradient is inversely proportional to the surface coverage, hence the change in slope indicates two different modes of coverage. Representative TEM images obtained for *n*-hexane droplets stabilised using G_{37}–H_{60}–B_{30} worms prepared at copolymer concentrations of (B) 1.0% w/w and (C) 0.1% w/w. A significantly higher worm surface coverage is observed when using the higher copolymer concentration (see image (B)).

concentration. At the lower copolymer concentration, the worms appear to adjust their surface packing density by forming 'islands', rather than individual worms becoming more evenly spaced. This cooperative behaviour allows them to stabilise somewhat smaller oil droplets than the equivalent spherical nanoparticles, while at the same time being much more strongly adsorbed at the oil–water interface. It is worth noting that these triblock copolymer linear worms are much more flexible than the bacterial cellulose nanofibres reported by Kalashnikova *et al.*[19] Thus it is the particle *anisotropy*, rather than the particle *stiffness*, that appears to be responsible for their strikingly similar Pickering emulsifier behaviour. In summary, the highly anisotropic character of these copolymer nanoparticles directly enhances their ability to act as an efficient Pickering emulsifier.

Conclusions

PISA offers a versatile and highly convenient route for the synthesis of a range of sterically-stabilised block copolymer nanoparticles with either spherical or worm-like morphologies in concentrated aqueous solution. In principle, such nanoparticles can act as novel Pickering emulsifiers for the stabilisation of oil-in-water emulsions. However, in practice the core-forming PHPMA block is only weakly hydrophobic, hence *linear* PGMA–PHPMA diblock copolymer nano-objects do not survive the high shear conditions required for homogenisation of the oil phase. This problem is observed for both spherical and worm-like copolymer morphologies. Fortunately, covalent stabilisation of both types of nanoparticles is readily achieved *via* chemical crosslinking with EGDMA, which enables their survival during emulsification. Whether such nanoparticles remain intact or undergo dissociation during homogenisation is readily assessed by examining the mean oil droplet diameter as a function of copolymer concentration. For soluble block copolymer chains, the mean droplet diameter exhibits essentially no concentration dependence, whereas the crosslinked nanoparticles exhibit strong concentration dependence (as expected for genuine Pickering emulsifiers). These findings are corroborated by TEM studies of colloidosome microcapsules prepared by introducing an oil-soluble polymeric crosslinker into the oil phase, since only those spherical or worm-like nanoparticles that were crosslinked prior to homogenisation are observed intact at the colloidosome surface. However, if the weakly hydrophobic PHPMA is either replaced or supplemented by a relatively hydrophobic core-forming block (*e.g.* PBzMA), the resulting linear spherical PGMA–PBzMA or worm-like PGMA–PHPMA–PBzMA nanoparticles are sufficiently stable to be utilised as Pickering emulsifiers. Hence chemical cross-linking is not mandatory for Pickering emulsification: sufficient stabilisation can be conferred simply by introducing stronger hydrophobic interactions between the core-forming blocks. Worm-like nanoparticles are shown to be much more effective Pickering emulsifiers compared to their spherical counterparts, since they are: (i) at least as *efficiently* adsorbed; (ii) almost certainly much more *strongly* adsorbed; and (iii) also *enable smaller droplets to be produced for a given nanoparticle concentration*. It appears that an anisotropic morphology also enables stable Pickering emulsions to be produced with relatively low surface coverage of the oil droplets when homogenisation is conducted at relatively low copolymer concentrations. Given the potentially scalable synthesis of these copolymer worms *via* RAFT-mediated PISA formulations, these findings suggest new research avenues for the rapidly-growing field of bespoke polymer-based Pickering emulsifiers.

Acknowledgements

EPSRC and The University of Sheffield are thanked for funding a Post-doctoral Prize Fellowship for KLT. SPA and KLT also acknowledge EPSRC for a Platform grant (EP/J007846/1) and SPA is a recipient of a five-year ERC Advanced Investigator grant (PISA 320372). SPA thanks Ashland (USA) for CASE support of an EPSRC PhD studentship for VJC.

Notes and references

1 S. U. Pickering, *J. Chem. Soc.*, 1907, **91**, 2001–2021.
2 W. Ramsden, *Proc. R. Soc. London*, 1903, **72**, 156–164.
3 Y. Cui, M. Threlfall and J. S. van Duijneveldt, *J. Colloid Interface Sci.*, 2011, **356**, 665–671.

4 S. A. F. Bon and P. J. Colver, *Langmuir*, 2007, **23**, 8316–8322.
5 S. Cauvin, P. J. Colver and S. A. F. Bon, *Macromolecules*, 2005, **38**, 7887–7889.
6 Y. Cui and J. S. van Duijneveldt, *Langmuir*, 2012, **28**, 1753–1757.
7 S. Levine, B. D. Bowen and S. J. Partridge, *Colloids Surf.*, 1989, **38**, 325–343.
8 B. P. Binks and S. O. Lumsdon, *Phys. Chem. Chem. Phys.*, 1999, **1**, 3007–3016.
9 B. P. Binks and S. O. Lumsdon, *Phys. Chem. Chem. Phys.*, 2000, **2**, 2959–2967.
10 B. P. Binks and C. P. Whitby, *Langmuir*, 2004, **20**, 1130–1137.
11 F. Gautier, M. Destribats, R. Perrier-Cornet, J.-F. Dechezelles, J. Giermanska, V. Heroguez, S. Ravaine, F. Leal-Calderon and V. Schmitt, *Phys. Chem. Chem. Phys.*, 2007, **9**, 6455–6462.
12 B. P. Binks and S. O. Lumsdon, *Langmuir*, 2001, **17**, 4540–4547.
13 B. P. Binks and S. O. Lumsdon, *Langmuir*, 2000, **16**, 8622–8631.
14 B. P. Binks, *Curr. Opin. Colloid Interface Sci.*, 2002, **7**, 21–41.
15 P. F. Noble, O. J. Cayre, R. G. Alargova, O. D. Velev and V. N. Paunov, *J. Am. Chem. Soc.*, 2004, **126**, 8092–8093.
16 B. Madivala, S. Vandebril, J. Fransaer and J. Vermant, *Soft Matter*, 2009, **5**, 1717–1727.
17 J. S. Guevara, A. F. Mejia, M. Shuai, Y.-W. Chang, M. S. Mannan and Z. Cheng, *Soft Matter*, 2013, **9**, 1327–1336.
18 I. Kalashnikova, H. Bizot, B. Cathala and I. Capron, *Biomacromolecules*, 2012, **13**, 267–275.
19 I. Kalashnikova, H. Bizot, B. Cathala and I. Capron, *Langmuir*, 2011, **27**, 7471–7479.
20 I. Kalashnikova, H. Bizot, P. Bertoncini, B. Cathala and I. Capron, *Soft Matter*, 2013, **9**, 952–959.
21 X. Zhang, S. Boisse, W. Zhang, P. Beaunier, F. D'Agosto, J. Rieger and B. Charleux, *Macromolecules*, 2011, **44**, 4149–4158.
22 S. Boisse, J. Rieger, K. Belal, A. Di-Cicco, P. Beaunier, M.-H. Li and B. Charleux, *Chem. Commun.*, 2010, **46**, 1950–1952.
23 Y. Li and S. P. Armes, *Angew. Chem., Int. Ed.*, 2010, **49**, 4042–4046.
24 A. Blanazs, J. Madsen, G. Battaglia, A. J. Ryan and S. P. Armes, *J. Am. Chem. Soc.*, 2011, **133**, 16581.
25 L. P. D. Ratcliffe, A. J. Ryan and S. P. Armes, *Macromolecules*, 2013, **46**, 769–777.
26 A. Blanazs, J. Madsen, G. Battaglia, A. J. Ryan and S. P. Armes, *J. Am. Chem. Soc.*, 2011, **133**, 16581–16587.
27 A. Blanazs, A. J. Ryan and S. P. Armes, *Macromolecules*, 2012, **45**, 5099–5107.
28 C. Grazon, J. Rieger, N. Sanson and B. Charleux, *Soft Matter*, 2011, **7**, 3482–3490.
29 *Polymer Handbook, 2nd edn.*, ed. J. Brandrup and E. H. Immergut, Wiley Interscience, New York, 1974.
30 S. Sugihara, A. Blanazs, S. P. Armes, A. J. Ryan and A. L. Lewis, *J. Am. Chem. Soc.*, 2011, **133**, 15707–15713.
31 M. Semsarilar, V. Ladmiral, A. Blanazs and S. P. Armes, *Langmuir*, 2011, **28**, 914–922.
32 K. L. Thompson, P. Chambon, R. Verber and S. P. Armes, *J. Am. Chem. Soc.*, 2012, **134**, 12450–12453.
33 P. Chambon, A. Blanazs, G. Battaglia and S. P. Armes, *Langmuir*, 2012, **28**, 1196–1205.
34 A. Blanazs, R. Verber, O. O. Mykhaylyk, A. J. Ryan, J. Z. Heath, C. W. I. Douglas and S. P. Armes, *J. Am. Chem. Soc.*, 2012, **134**, 9741–9748.
35 V. J. Cunningham, A. M. Alswieleh, K. L. Thompson, M. Williams, G. J. Leggett and S. P. Armes, *Macromolecules*, 2014, **47**, 5613–5623.
36 M. K. Kocik, O. O. Mykhaylyk and S. P. Armes, *Soft Matter*, 2014, **10**, 3984–3992.
37 K. L. Thompson, S. P. Armes, J. R. Howse, S. Ebbens, I. Ahmad, J. H. Zaidi, D. W. York and J. A. Burdis, *Macromolecules*, 2010, **43**, 10466–10474.
38 J. A. Balmer, S. P. Armes, P. W. Fowler, T. Tarnai, Z. Gaspar, K. A. Murray and N. S. J. Williams, *Langmuir*, 2009, **25**, 5339–5347.
39 O. J. Cayre, J. Hitchcock, M. S. Manga, S. Fincham, A. Simoes, R. A. Williams and S. Biggs, *Soft Matter*, 2012, **8**, 4717–4724.
40 M. G. Basavaraj, G. G. Fuller, J. Fransaer and J. Vermant, *Langmuir*, 2006, **22**, 6605–6612.
41 B. Madivala, J. Fransaer and J. Vermant, *Langmuir*, 2009, **25**, 2718–2728.
42 J. Madsen, S. P. Armes and A. L. Lewis, *Macromolecules*, 2006, **39**, 7455–7457.
43 In this particular case, relatively non-spherical *n*-dodecane droplets were produced, whereas spherical droplets were obtained for each of the other five Pickering emulsions. The former observation is reproducible but not currently understood. However, we note that spherical droplets can be achieved by using alternative oils (*e.g.* sunflower oil) – see ref. 35.